

# An absolute interface coordinates floating frame of reference formulation for plates

M. van den Belt<sup>1</sup>, J.P. Schilder<sup>1</sup>, D.M. Brouwer<sup>1</sup>

<sup>1</sup> University of Twente, Faculty of Engineering Technology  
P.O. Box 217, 7500AE Enschede, The Netherlands  
e-mail: [m.vandenbelt@utwente.nl](mailto:m.vandenbelt@utwente.nl)

## Abstract

In this work, a recently developed superelement formulation in the floating frame of reference is implemented for plates. By using Craig-Bampton modes, a coordinate transformation from the absolute floating frame coordinates and local elastic coordinates to the absolute interface coordinates is established. Several benchmark problems are considered to validate the formulation for plates. Results from the superelement formulation for plates are in good agreement with other formulations, meaning that the formulation can successfully be used for the efficient description of plates in flexible multibody systems, such as flexure mechanisms that can no longer be modelled as beam elements because of their unbeamlike dimensions.

## 1 Introduction

In precision engineering, flexure hinges are frequently used for their deterministic behavior, due to the absence of friction, hysteresis, and backlash [2]. Flexure hinges allow motion by being compliant in driving directions, while constraining motion in other directions, as shown in Figure 1. Generally, as the support stiffness rapidly decreases with deflection, flexure hinges have a reduced performance in their deflected state [2]. Shape and topology optimization is used to design sophisticated mechanisms to minimize this performance reduction. This requires modelling the flexure mechanisms with computer simulations.

As these forms of optimization require many design evaluations, reduction of computational costs is desired. To decrease the computational costs, flexures are often simplified as flexible multibody systems using nonlinear beam elements. This is a valid assumption as long as the flexures are long and slender, and thus have a high aspect ratio (defined as length/height).

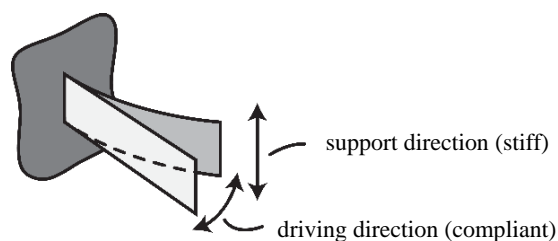


Figure 1 Single leaf spring flexure.

Flexible multibody dynamics concerns the study of mechanisms that consist of multiple deformable bodies. These deformable bodies are attached to each other or to the fixed world at their interface points. The problem is geometrically nonlinear as the joints at the interface points allow for large rigid body rotations. However, because the elastic deformations within a body are considered to remain small, linear elasticity

theory can be used. For the simulations of such systems, general suitable formulations can be classified into three categories: the inertial frame formulation, the corotational formulation, and the floating frame formulation. In each formulation, kinematics and kinematic constraints are described differently. The kinematics of a body represent its motion, which is described by the motion of coordinate frames that are rigidly attached to different material points on the body. Kinematic constraints represent the connections between bodies, and relate the motions of the coordinate frames at the interface points of different bodies.

The inertial frame formulation is a nonlinear finite element formulation, using the nonlinear Green-Lagrange strain definition [3]. By using global interpolation functions, each body is discretized into finite elements. The degrees of freedom in this formulation are the absolute nodal coordinates. Kinematic constraints are easily enforced by equating nodal coordinates of the interface points between the different bodies. The inertial frame formulation does not make a distinction between large rigid body rotations and small elastic deformations.

The corotational frame formulation can be regarded as an extension of the linear finite element formulation [4, 5]. A corotational coordinate frame describes large rigid body motions of elements with respect to an inertial frame. Small deformations are then superimposed using linear finite element matrices, based on the Cauchy strain definition [6]. Nonlinear finite element models are obtained by pre- and post-multiplying element matrices with rotation matrices based on the corotational frame. As in the inertial frame formulation, absolute nodal coordinates are the degrees of freedom, and as such, constraints are obtained in the same way. The corotational frame formulation does not distinguish between flexible and rigid bodies, which makes the simulation of models containing rigid bodies less efficient.

The floating frame formulation can be interpreted as a flexible extension on rigid multibody formulations [7]. In this formulation a floating frame describes a body's large rigid body motions and a linear combination of mode shapes is used to describe local elastic deformations. Since the local deformations remain small, these mode shapes can be obtained by applying powerful model order reduction techniques on a body's linear finite element model [7]. The absolute floating frame coordinates and the local generalized coordinates corresponding to the mode shapes are the degrees of freedom of the system. As the interface points are not part of the degrees of freedom, the kinematic constraints are in general nonlinear. Therefore, Lagrange multipliers are required to enforce the kinematic constraints, increasing the number of degrees of freedom and subsequently the computational costs.

As the floating frame formulation allows for well-developed model order reduction techniques, this is the preferred formulation in many multibody systems where the elastic deformation within a body remains small. Recent research presented a method that overcomes the disadvantage of having to introduce Lagrange multipliers [1]. By using Craig-Bampton modes [8], a coordinate transformation from the absolute floating frame coordinates and local elastic coordinates to the absolute interface coordinates is established. The coordinate transformation is used to create so-called superelements in the floating frame formulation. This way, the Lagrange multipliers are eliminated and as the interface coordinates are now part of the degrees of freedom, kinematic constraints can be enforced in the same straightforward way as in inertial frame formulation. In this way, the new superelement formulation combines the advantages of the different formulations mentioned above.

Within precision engineering, recent developments of flexure mechanisms are aimed at the optimization of mechanisms with a high support stiffness while heavily loaded in supporting directions; whereas, state-of-the-art optimizations are mostly aimed at high support stiffness during a large range of motion [9]. In the latter case, flexure mechanisms can often be simplified as beam elements. However, flexure mechanisms that are loaded in their supporting direction typically are short and wide instead of long and slender, meaning that they have a low aspect-ratio instead of a high one. This implies that the mechanisms can no longer be simplified as beam elements, as they do not provide sufficient accuracy. Plate elements should be used instead of beam elements to obtain sufficient accuracy; however, this increases the number of degrees of freedom and therefore computational costs significantly.

The method presented by Ellenbroek and Schilder offers a promising reduction method for these types of problems [1]. The method is applicable for the reduction of arbitrarily shaped bodies, although the original work only presented validation problems with beams. In this work, superelements are implemented in the floating frame formulation for plates. Benchmark problems for plates are considered to extend this

validation. To this end, a cantilever and a clamped square plate are modelled. The cantilever is loaded at the free tip, whereas the clamped square plate is loaded with a point load on the centerline of the plate. Simulation results are compared to results obtained using both the corotational frame formulation and the inertial frame formulation. This way, validity of the superelements in the floating frame formulation are validated against other formulations as well.

The paper is structured as follows: Chapter 2 of this paper presents an overview of the essentials of the method presented by Ellenbroek and Schilder [1]. In Chapter 3, this method will be applied to plates; kinematics for plates in the floating frame are discussed, as well as its implementation in the new superelement method. In Chapter 4, two validation examples are considered: a cantilever and a clamped square plate. These examples are adapted from Izzuddin [10]. Conclusions are discussed in Chapter 5 and this paper is concluded with recommendations for further research in Chapter 6.

## 2 Absolute interface coordinates in the floating frame formulation

To describe the kinematics of a plate in the regular floating frame formulation, the coordinates of each interface point are expressed in terms of the absolute floating frame coordinates and the local interface coordinates. This is shown graphically in Figure 2.

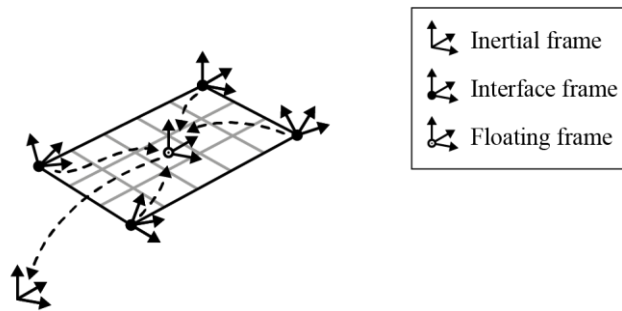


Figure 2 Floating frame formulation for a plate.

Different choices can be made for the set of deformation shapes that describe the local elastic deformations. However, as the local interface coordinates are in fact the generalized coordinates corresponding to static Craig-Bampton modes, it is natural to choose these as the deformation shapes. This way, the coordinate transformation towards absolute interface coordinates can be established. However, since both the Craig-Bampton modes and the floating frame coordinates are able to describe rigid body modes, these modes need to be eliminated from the Craig-Bampton modes. This is realized by defining the floating frame such that there is zero elastic deformation at its location. Both the coordinate transformation and the way the constraints are satisfied are described in detail in [1]. Using the coordinate transformation, the equation of motion and the equilibrium equation can be rewritten from the standard floating frame to the new coordinate set. As Chapter 3 only addresses static examples, the equilibrium equations are of more relevance here. The equilibrium equation in standard floating frame form is given by:

$$\mathbf{Kq} = \mathbf{F}, \tag{1}$$

where  $\mathbf{K}$  is the global stiffness matrix according to the floating frame formulation,  $\mathbf{q}$  is the vector of generalized coordinates and  $\mathbf{F}$  contains the generalized forces that are externally applied or due to kinematic constraints. The equilibrium equation after the coordinate transformation is given by:

$$[\mathbf{R}][\mathbf{T}]^T \mathbf{K}_{CB} \mathbf{q}_{LI} = \mathbf{F}, \tag{2}$$

where  $[\mathbf{R}]$  contains the rotation matrices that relate the floating frame to the inertial frame.  $\mathbf{K}_{CB}$  is the stiffness matrix that is obtained by model order reduction of the body's finite element model, using the Craig-Bampton modes and  $\mathbf{q}_{LI}$  are the local interface coordinates. Finally,  $[\mathbf{T}]$  is a transformation matrix that removes the rigid body motion of the floating frame from the expression.  $[\mathbf{T}]$  is given by:

$$[\mathbf{T}] = \mathbf{1} - [\Phi_{rig}][\mathbf{Z}], \quad (3)$$

in which  $[\Phi_{rig}]$  contains the displacement of all interface coordinates when the body is subjected to a rigid body motion with respect to the floating frame. The matrix  $[\mathbf{Z}]$  is given by:

$$[\mathbf{Z}] = ([\Phi_{CB}][\Phi_{rig}])^{-1}[\Phi_{CB}], \quad (4)$$

where  $[\Phi_{CB}]$  consists of the Craig-Bampton mode shapes evaluated at the floating frame. This equilibrium equation is the basis of the examples discussed in Chapter 3. Further details of the coordinate transformation and derivations are presented in [1].

### 3 Validation

To verify validity of the proposed formulation for plates, two static problems are modelled. First, a cantilever that is loaded out-of-plane is considered. Its dimensions are such that beam theory is still valid and therefore the results are also compared to formulations for beams. Second, a square plate is considered that is clamped on two opposite sides. Both examples are adapted from [10].

#### 3.1 Cantilever

In the first example, a cantilever is modelled. The cantilever, shown in Figure 3, is loaded in positive transverse ( $z$ -)direction. The cantilever has length  $L = 10 \text{ m}$ , width  $w = 1 \text{ m}$ , and thickness  $t = 0.1 \text{ m}$ . It has a Young's modulus of  $E = 12 \text{ GPa}$  and a Poisson ratio of  $\nu = 0.3$ . A mesh of 10 elements is used for all simulations and the load is modelled as two equal point loads at the two nodes at the cantilever tip. The response of the tip in both  $x$ - and  $z$ -direction is measured.

The problem is modelled using the superelement formulation for plates and is compared to three other formulations. The results for the superelement formulation implemented for plates are represented by the black solid line in Figure 4. The grey solid line represents the problem modelled in Ansys (shell181 elements), using a nonlinear finite element formulation based on the full nonlinear Green-Lagrange strain expression [3]. As the cantilever is long and slender, and thus has a high aspect-ratio, simplifying it as beam elements is allowed. To this end, the superelement formulation for beams is also used for validation, as well as the corotational formulation using nonlinear beam elements from software package Spacar. The latter two are represented by, respectively, black and grey dashed lines. The detailed formulation of Spacar can be found in [11].

Figure 4 shows the normalized transverse ( $w/L$ ) and axial ( $-u/L$ ) displacements. This figure shows that there is a favorable comparison between the four methods. Maximum deviations from Ansys are in the range of approximately 1 to 3%. Furthermore, there is a clear resemblance between Figure 4 and the results from Izzuddin (Figure 8 from [10]).

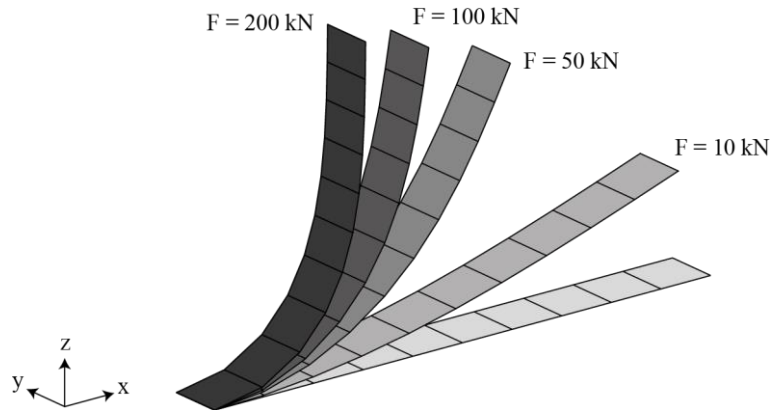


Figure 3 Deflected shapes of cantilever for different loads.

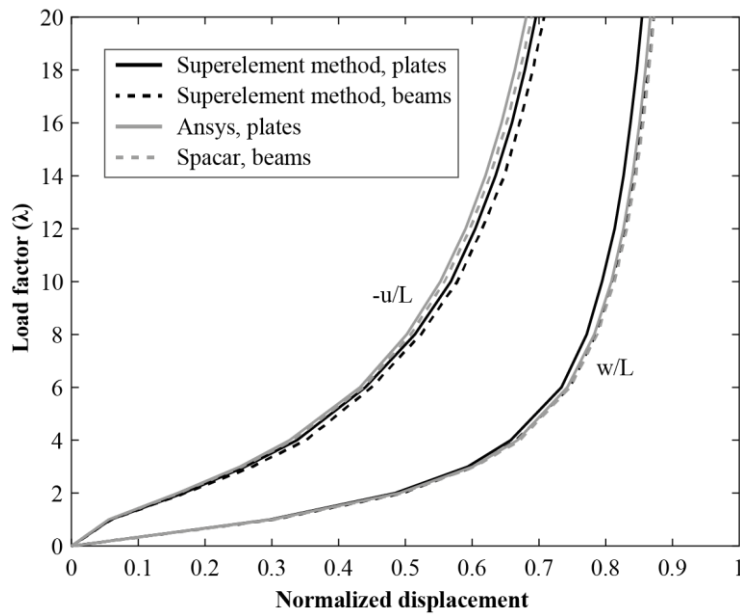
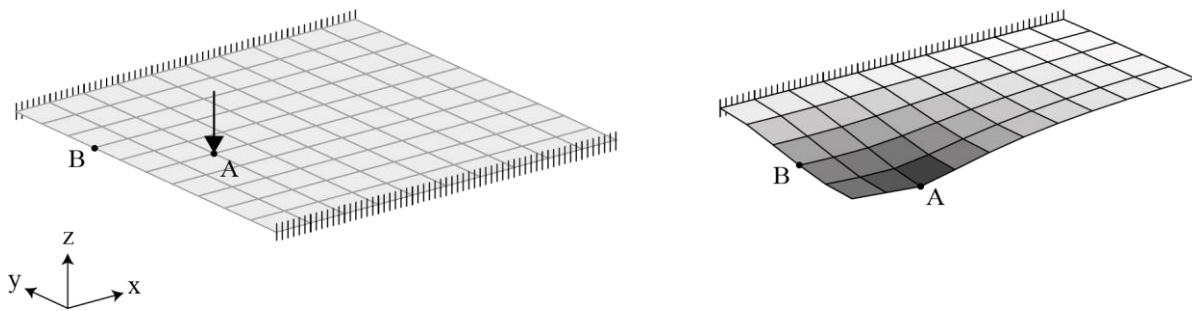


Figure 4 Response of cantilever to tip point loading.

### 3.2 Clamped square plate

In the second example, a square plate is modelled and loaded by a point load  $P$ . The plate has length and width  $L = w = 400 \text{ mm}$  and thickness  $t = 1.98 \text{ mm}$ . Its Young's modulus is  $E = 21.5 \text{ GPa}$  and its Poisson ratio is  $\nu = 0.3$ . The plate is clamped on two opposite edges. Figure 5 shows the plate (left) as well as shows the deflected shape (right). For clarity reasons, only half of the deflected plate is shown and displacements are scaled with a factor 10. A mesh of  $10 \times 10$  elements is used. The point load is applied at node A (Figure 5) which lies on the center line, at the third node from the free edge. The  $z$ -displacement at this node, as well as at node B, is measured. As this problem cannot be modelled using beam elements, the results are compared with software package Ansys only.

Figure 6 shows the results for displacements in the order of the thickness of the plate ( $P = [0, 25]$  N). As can be seen, both methods correspond very well. For a point load of 25 N, the deviation is approximately 1 to 2%. If the load is increased up to 250 N, the deviation also slightly increases, with a maximum deviation of slightly over 3% for the displacement of node B. The results for the load range  $P = [0, 250]$  N are presented in Figure 7. Results for both load ranges are also in close agreement with the results from Izzuddin (Figures 10 and 11 from [10]).



**Figure 5** Clamped square plate (left) and deflected shape for  $P = 250$  N (right, displacement scale = 10).

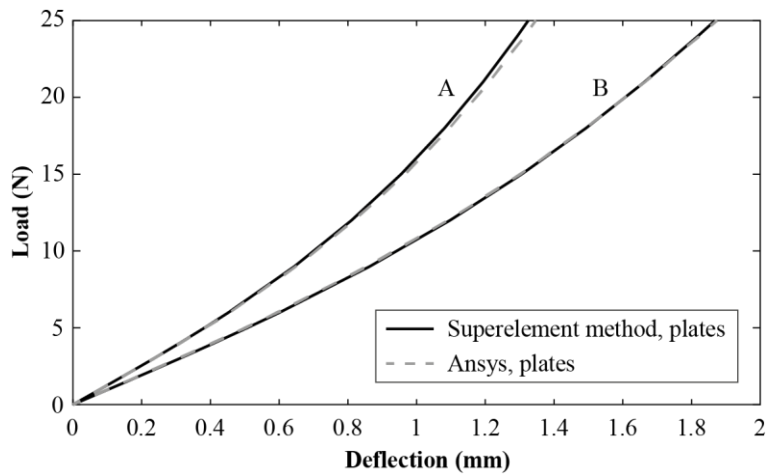


**Figure 6** Response of nodes A and B on clamped square plate for  $P = [0, 25]$  N.

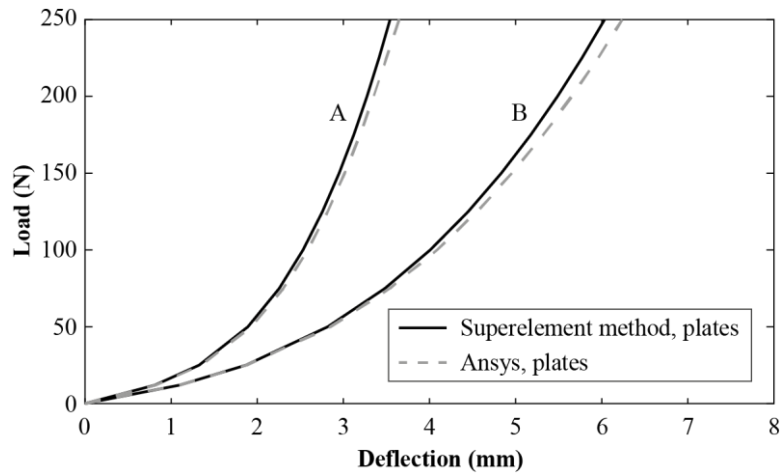


Figure 7 Response of nodes A and B on clamped square plate for  $P = [0, 250]$  N.

## 4 Discussion

Examples in Chapter 3 showed that the results from the superelement formulation for plates are in good agreement with the other formulations. This means that the method can successfully be used for the efficient description of plates in flexible multibody dynamics. However, some small deviations of around 1 to 3% still occur.

The small deviation is probably caused by the way the location of the floating frame is determined. It is known that the elastic displacements in the interface coordinates, multiplied by the Craig-Bampton mode shapes, should always equal zero at the location of the floating frame. However, a numerical error may cause this relation to be non-zero, and thus cause the floating frame to drift away. Therefore the location becomes slightly inaccurate after a while. This problem is expected to be solved by determining the location of the floating frame using a Newton-Raphson procedure. The Newton-Raphson procedure should be applied on the multiplication of the elastic displacements in the interface coordinates and the Craig-Bampton mode shapes, which should finally equal zero. The position of the floating frame at the current time step can be used as an initial estimate. In future work, this Newton-Raphson procedure will be implemented.

As the method is successfully implemented for plates, the method offers a promising reduction method for flexure mechanisms. Flexures that can no longer be simplified as beam elements, because of their low aspect-ratio, can be modelled in an accurate way using superelements.

## Acknowledgements

This research was funded by the Netherlands Organisation for Scientific Research (14665 NWO TTW) of the Ministry of Education, Culture and Science of the Netherlands.

## References

- [1] M.H.M. Ellenbroek, J.P. Schilder. *On the use of absolute interface coordinates in the floating frame of reference formulation for flexible multibody dynamics*. Multibody System Dynamics (2017). <https://doi.org/10.1007/s11044-017-9606-3>
- [2] K. Gunnink, R.G.K.M. Aarts, D.M. Brouwer. *Performance optimization of large stroke flexure hinges for high stiffness and eigenfrequency*, in *Proceedings of the 28th Annual Meeting of the American Society for Precision Engineering (ASPE), 2013 October 20-25*, Saint Paul, Minnesota, USA: American Society for Precision Engineering.
- [3] R. de Borst, M.A. Crisfield, J.J.C. Remmers, C.V. Verhoosel. *Non-Linear Finite Element Analysis of Solids and Structures, 2nd edn*, John Wiley & Sons, Ltd, New York (2012).
- [4] C.C. Rankin, F.A. Brogan. *An Element Independent Corotational Procedure for the Treatment of Large Rotations*. J. Pressure Vessel Technol, Vol. 108, No. 2 (1986), pp. 165-174.
- [5] M.A. Crisfield. *A consistent co-rotational formulation for non-linear, three-dimensional, beam elements*. Computer Methods in Applied Mechanics and Engineering, Vol. 81, Issue 2 (1990), pp. 131-150.
- [6] A. Kaye, R.F.T. Stepto, W.J. Work, J.V. Alemán, A. Ya. Malkin. *Definition of terms relation to the non-ultimate mechanical properties of polymers*. Pure and Applied Chemistry, Vol. 70, Issue 3 (1998), pp 701-754.
- [7] A.A. Nada, B.A. Hussein, S.M. Megahed, A.A. Shabana. *Use of the floating frame of reference formulation in large deformation analysis: experimental and numerical validation*. Proceedings of the Institution of Mechanical Engineers, Part K: Journal of Multi-body Dynamics, Vol. 224, Issue 1 (2010), pp. 45-58.
- [8] R.R. Craig, M.C.C. Bampton. *Coupling of substructures for dynamic analysis*, AIAA Journal, Vol. 6, No. 7 (1968), pp. 1313-1319.
- [9] M. Naves, D.M. Brouwer, R.G.K.M. Aarts. *Building block based spatial topology synthesis method for large stroke flexure hinges*, Journal of mechanisms and robotics, Vol 9, Issue 4 (2017), [041006].
- [10] B.A. Izzuddin, *An enhanced co-rotational approach for large displacement analysis of plates*. International Journal for Numerical Methods in Engineering, Vol 64, Issue 10, John Wiley & Sons, Ltd (2005), pp. 1350-1374.
- [11] J.B. Jonker, J.P. Meijaard. *A geometrically non-linear formulation of a three-dimensional beam element for solving large deflection multibody system problems*, International journal of non-linear mechanics, Vol. 53 (2013), pp. 63-74.